BJR

INSTRUCTIONAL REVIEW: RESEARCH

MRI of articular cartilage at microscopic resolution

Y. Xia

From Oakland University, Rochester, Michigan, United States

This review briefly summarises some of the definitive studies of articular cartilage by microscopic MRI (μMRI) that were conducted with the highest spatial resolutions. The article has four major sections. The first section introduces the cartilage tissue, MRI and μMRI, and the concept of image contrast in MRI. The second section describes the characteristic profiles of three relaxation times (T_1, T_2 and $T_{1\rho}$) and self-diffusion in healthy articular cartilage. The third section discusses several factors that can influence the visualisation of articular cartilage and the detection of cartilage lesion by MRI and μMRI. These factors include image resolution, image analysis strategies, visualisation of the total tissue, topographical variations of the tissue properties, surface fibril ambiguity, deformation of the articular cartilage, and cartilage lesion. The final section justifies the values of multidisciplinary imaging that correlates MRI with other technical modalities, such as optical imaging. Rather than an exhaustive review to capture all activities in the literature, the studies cited in this review are merely illustrative.

Keywords: MRI, Microscopic resolution, Articular cartilage, Osteoarthritis, Depth-dependent profiles, Image contrast, Relaxation times, Self-diffusion, Image analysis strategy, Imaging artefact

Introduction

The gradual degradation of articular cartilage is a hallmark of osteoarthritis (OA), a major musculoskeletal disease that contributes to the number one cause of disability in adults.[1-3] Anatomically, articular cartilage is a thin layer of connective tissue covering the load bearing ends of bones in joints to absorb shocks and distribute loads. While the structure and properties of healthy and diseased cartilage have been studied extensively, an accurate diagnosis of early OA in humans, at a stage when a clinical intervention might potentially be useful, remains elusive in practice.[4] The early diagnosis has two main obstacles: 1) the early changes in the tissue's fine structure and delicate functions markedly precede the development of OA as a clinical disease; and 2) current diagnostic imaging has insufficient resolution and unsatisfactory sensitivity to detect early (i.e., small) lesions in cartilage.

In order to overcome the first obstacle, animal models of the human disease have been established. Since OA is a slow-progression disease spanning many years, the disease remains silent at the early stages. When a patient presents to a clinic, it is usually due to complaining of pain in the joints – unfortunately, pain correlates poorly with what the cartilage looks like, whether histologically, arthroscopically, radiologically or on MRI.[5-9] As one cannot initiate a disease in humans, and is it not possible to test some potential disease-modification drugs on humans before the drugs' effectiveness is demonstrated, animal models serve an essential purpose in human biomedical research. Once we understand the degradation of tissue from the very beginning (the most vital period) to the end, step-by-step, in animal models, an intervention at the early stages before the point-of-no-return could be designed to eventually save human joints.

In order to overcome the second obstacle, one must have high-resolutions in any diagnostic imaging.[10] This is because articular cartilage contains complex, depth-dependent structures and localised progression of disease across its thin thickness. Since MRI is the only totally non-invasive imaging tool with excellent soft-tissue contrast, microscopic MRI (μMRI) is the logical bridge that would be able to translate the findings between invasive procedures (e.g., light microscopy or biochemical assay) and clinical MRI diagnostics. As there is no difference in physics principles and engineering architectures between μMRI and clinical MRI, there exists

Y. Xia, PhD, Professor of Medical Physics
Oakland University, 276 Hannah Hall, Department of Physics, Rochester, Michigan 48309, USA.

Correspondence should be sent to Professor Y. Xia; e-mail: xia@oakland.edu

10.1302/2046-3758.21.2000135
$2.00

Bone Joint Res 2013;2:9–17.

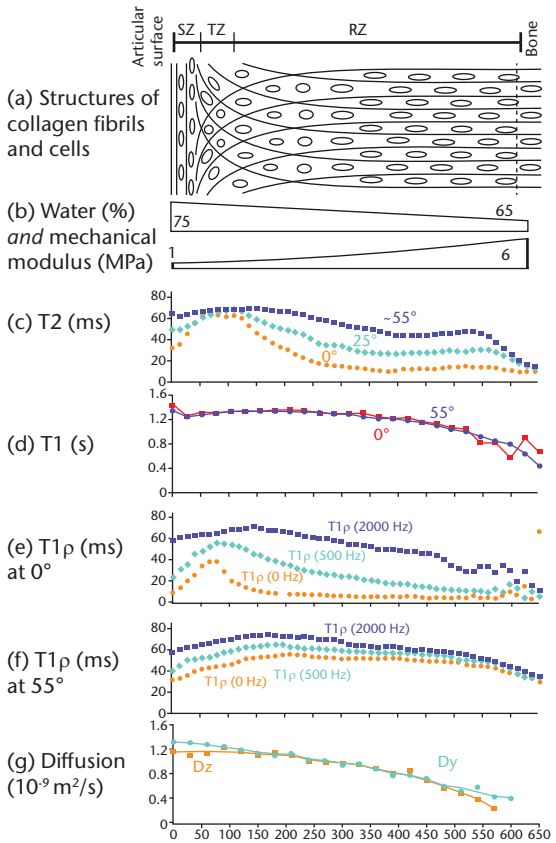

Fig. 1

The depth-dependent structures and properties of canine humeral articular cartilage by μMRI. Figure 1a – schematic diagram of cartilage showing the orientation of the collagen fibrils (the short lines) in different histological zones and the orientation of the chondrocytes (the circles and ovals) (not to scale). Figure 1b – approximate water concentration and depth-dependent compressive modulus in cartilage. Figure 1c – T_2 anisotropy profiles of articular cartilage at different specimen orientations (0° is when the articular surface is perpendicular to the magnetic field direction). Figure 1d – T_1 profiles of articular cartilage at two specimen orientations. Figures 1e and 1f – $T_{1\rho}$ profiles of articular cartilage under three different spin-lock powers e) at 0° and f) at 55°. Figure 1g – self-diffusion profiles of articular cartilage when the diffusion gradient is applied in the two different directions.

no fundamental obstacle that will prevent the realisation of higher resolutions in clinical MRI scanners.[10,11] Since the tissue or organ in common animal models are smaller than human tissues and organs, and since the goal of any biomedical research is to identify the early lesion, the use of high-resolution μMRI in animal studies is an effective and logical strategy to identify the parameter or procedure that might be clinically useful.

This review briefly summarises some of the definitive studies of articular cartilage by μMRI that have the highest spatial resolutions. Rather than an exhaustive review to capture all activities in the literature, the studies cited are merely illustrative. The interested readers can easily find additional readings and many equally important studies with a key-word search.

Articular cartilage

Articular cartilage in large animals and humans contains a scattered population of living cells (chondrocytes), which accounts for 1% to 2% of the total tissue.[12] Most of the cartilage is extracellular and composed primarily of three molecules: water (approximately 70%), collagen (approximately 20%) and proteoglycan (approximately 5%).[13,14] The collagen in the tissue is primarily type II triple-helical fibrils that form a 3D matrix.[15] The proteoglycan (PG) has a bottle-brush-like structure with numerous side-chains of sulfated glycosaminoglycans (GAGs).[16] Structurally, articular cartilage is highly ordered and is commonly considered to comprise three sub-tissue zones based on the local orientation of the collagen fibrils (Fig. 1a).[17,18] These three zones are the superficial zone (SZ) where the collagen is orientated parallel with the articular surface, the transitional zone (TZ) where the collagen is orientated rather randomly, and the radial zone (RZ) where the collagen is orientated perpendicularly to the articular surface. In addition, many of the biological and physical properties of articular cartilage are also known to be depth-dependent (Fig. 1b).[13,14,16,19]

It should be noted, however, that the common definition of these 'sub-tissue zones' is only a concept, not a clearly defined reality.[19] Anyone who uses a high-resolution imaging tool to examine a piece of articular cartilage would not find any sharp 'line' or 'border' across which the property of tissue differs distinctively. Instead, the tissue changes gradually over a finite distance, which yields a continuous function of tissue properties. Consequently, any criterion to truncate the continuous function into several discrete zones is intrinsically arbitrary and model-dependent.[19] The concept of these 'discrete zones', however, is a useful one in terms of focusing attention to a particular portion of tissue.

MRI and μMRI. The principles of nuclear magnetic resonance imaging (NMR Imaging or MRI) are well understood. At the heart of the technique is the linear proportionality between the precessional frequency of the nuclei (e.g., protons in water) and the magnitude of the external magnetic field in which the nuclei are immersed. By making the magnetic field deliberately non-uniform (commonly a linear gradient), the frequency of these nuclei will differ from one location to another across the sample. The location of the nuclei is, therefore, encoded by a shift of their precessional frequencies. By setting up three gradient fields in three orthogonal directions, the nuclei (or water molecules) can be spatially encoded in any 3D or 2D space.

With the scaling down of the receiver coil and fine-tuning of the instrument, the resolution of MRI could be as fine as 10 μm. When the size of one volume element (voxel) of the image is < 100 μm, MRI is termed NMR microscopy (microscopic MRI, or μMRI).[11,20-22] μMRI is exceptionally well suited for the study of spatially heterogeneous biological materials in animal models because of

its high sensitivity to the molecular environments. The ability to produce microscopic-resolution images of molecular-level environments and activities distinguishes μMRI from other microscopic imaging methods such as ultrasound or CT. The fact that μMRI shares identical physics principles and engineering architectures with clinical MRI ensures the direct relevance of the μMRI results to clinical MRI research. Since the proton (^{1}H) is the most common nucleus in biological systems, and also the most sensitive nucleus among all nuclear species, the majority of MRI experiments are carried out to measure the protons in water molecules. In articular cartilage, MRI essentially measures extracellular matrices (the cells are invisible in MRI), where the depth-dependent characteristics of the collagen matrix play the foremost role.

Concept of MRI contrast. The exquisite sensitivity of MRI signals to molecular motion and molecular dynamics is the true value of this non-destructive and non-invasive imaging technique, a technique that can best be understood in terms of image contrasts.[11] There are several fundamental mechanisms in MRI contrasts. For example, if the molecule moves physically from one location to another during an imaging experiment (such as the blood flow in animal or human, or vascular flow in plants), the MRI signal will carry an extra phase shift associated with the flowing molecule. The molecule's velocity can be quantified in the subsequent image analysis.[23,24] Another example relates to the time delay for the molecules when they are excited and sampled, which will manipulate the MRI signal with a complex attenuation that can also be quantified. In principle, it is difficult to acquire a map of the true water density in MRI, as any image in MRI is always weighted by several intrinsic image contrasts regardless of whether the experimentalist intends to image the contrast or not. A perfect example of this type of unwanted image contrast is the 'magic angle effect' in MRI of cartilage[25]; this effect has an orientation-dependent inconsistency between the known water content and the image intensity of the specimen.

Three relaxation times are the most important in MRI of cartilage. They are T_1 (the spin-lattice relaxation time), T_2 (the spin-spin relaxation time), and $T_{1\rho}$ (the spin-lattice relaxation time in the rotating frame). The fundamental principles of spin relaxation in MRI reside deep in NMR physics and are beyond the scope of this review. In essence, these relaxation times are closely related to different frequencies of the molecular dynamics. It can be shown that T_1 is sensitive to the highest frequencies of molecular motions, or frequencies close to the precessional frequencies in the MHz range; $T_{1\rho}$ is sensitive to the intermediate frequencies of molecular motions, probably in several or tens of kHz; and T_2 is sensitive to the lowest frequencies of molecular motions involving static or slowly fluctuating magnetic fields.[26]

A subtle feature of the relaxation time measurement in biological systems is the possible dependency of their values on the specimen orientation in the external magnetic field, where the relaxation times are said to have anisotropy. The main cause of the relaxation anisotropy is the dipolar interaction between the water molecules and the (less mobile) macromolecules in the tissue. In addition, the exchange between different molecular environments and cross relaxation between protein macromolecules and water are important aspects of the relaxation mechanism in biological materials. For articular cartilage, T_1 relaxation was found to be isotropic while T_2 relaxation was found to have a strong orientational dependence that varied as $(3\cos^2\theta - 1)$,[27] the geometrical factor that dominates the non-zero dipolar Hamiltonian. These characteristics are the indications of slow macromolecular motion in cartilage, likely related to the highly constrained motion of swollen proteoglycans in the collagen matrix.[28]

In addition to three relaxation times, several other MRI parameters can also cause the image contrast of cartilage in MRI, including self-diffusion (D) and magnetisation transfer (MT). Self-diffusion measures the random Brownian motion, a motion that results in the loss of the MRI signal amplitude and can be quantified with the use of specific imaging sequences. The diffusion images from articular cartilage also have some anisotropy,[29] which is weaker than the T_2 anisotropy in cartilage. Since D and MT are smaller effects than the relaxation times are, measurements of self-diffusion and magnetisation transfer are less common in the MRI of cartilage.

Experimentally, since the images from MRI are intrinsically weighted by some of these image contrast factors, one can use specific pulse sequences to purposely acquire a weighted image (e.g., T_1- or T_2-weighted). Alternatively, one can acquire a series of images, each weighted by the same contrast factor but by a different amount. A subsequent pixel-by-pixel calculation can construct a parameter image, such as a T_1 or T_2 image. The practice of calculating the parameter images has become common clinically.

Characteristics of articular cartilage by MRI at microscopic resolution

It has been known for two decades that normal (i.e., healthy) articular cartilage can appear laminated in MRI when the tissue is placed at certain orientations with respect to the external magnetic field.[25,30-33] In other words, instead of having a uniform intensity, several thin sub-layers that are parallel with the articular surface (the surface of the tissue) can be seen inside the cartilage. Each of the sub-layers has a different intensity and thickness.[31,33,34] When the tissue surface is placed at about 55° with respect to the main magnetic field, the tissue intensity can become homogeneous and higher than at other angles. Since 54.57° is known as the magic angle in MRI physics, this laminar appearance of articular cartilage is also known as the magic angle effect of cartilage in MRI literature.[35-37]

T_2 relaxation. The origin of the magic angle effect in MRI of cartilage soon became clear with the discovery of T_2 anisotropy in articular cartilage in the mid-1990s. In essence, T_2 in articular cartilage is both depth-dependent and orientation-dependent, as shown in Figure 1c.[27,38] These features of T_2 anisotropy were immediately interpreted as being caused mainly by the depth-dependent structure of the collagen matrix in cartilage,[25] which imposes a depth-dependent motional anisotropy for the protons in the tissue due to their close interaction with the collagen matrix. A set of quantitative criteria was soon developed in a combined μMRI and polarised light microscopy study that successfully divided the tissue into three MRI zones, which were statistically equivalent to the three histological zones in cartilage.[39] This equivalency between the μMRI zones and histological zones is important because it demonstrates that just as noncalcified cartilage can be conceptually subdivided based on the orientation of the collagen fibers into three distinct structural zones in histology, in μMRI, a piece of articular cartilage can also be subdivided based on the regional characteristics of T_2 relaxation into three structural zones. This enables multidisciplinary research of cartilage.

T_1 relaxation. In contrast to the strong T_2 anisotropy in articular cartilage, T_1 in articular cartilage is known to be isotropic to the magnetic field direction and has only a small dependency on its tissue depth, as shown in Figure 1d.[25,40] This isotropic T_1 and anisotropic T_2 in healthy cartilage tissue indicate precisely the very slow motion of the water molecules, which came from the highly constrained proteoglycans in cartilage (hence the lack of high frequency motions). In most imaging experiments, therefore, T_1 itself would cause few complications in MRI of articular cartilage. Recently, a laminar appearance that had the opposite intensity pattern was observed in MRI of cartilage by using some fast imaging sequences.[41] This reversed laminae was attributed to the small reduction of T_1 in the deep tissue (Fig. 1d), which causes the intensity elevation of the deep tissue in MRI, a phenomenon noted earlier as "uncertain etiology" by McCauley and Disler.[42] This reversed laminae in cartilage reminded us that the underlying molecular structure in cartilage and the imaging methodology should both be considered when one examines the appearance of cartilage in MRI.

The usefulness of T_1 relaxation in MRI of cartilage came from the development of the dGEMRIC (delayed Gadolinium Enhanced Magnetic Resonance Imaging of Cartilage) protocol in MRI. This protocol doped the tissue with the $Gd(DTPA)^{2-}$ contrast agent. Since these charged ions distribute in the cartilage in an inverse relation compared to the concentration of the negatively charged GAG molecules, and since gadolinium is a paramagnetic ion that shortens the T_1 relaxation, a GAG image can be constructed based on two T_1 images acquired before and after the patient is injected with the Gd contrast agent.[43-48] This dGEMRIC procedure has become important in the clinical detection and management of joint diseases, since the reduction of GAG in tissue will result in a biochemically and biomechanically weakened cartilage, an early sign of the tissue degradation. A set of high-resolution GAG profiles was obtained in μMRI,[49] which shows that the GAG concentration in canine cartilage is approximately a linear function, increasing from the superficial zone to the radial zone. One peculiar feature in the original dGEMRIC protocol was an arbitrary scaling constant of two,[43] which was needed to make the experimental values between MRI and histochemistry agree with each other. This arbitrary scaling factor was recently found to be unnecessary.[50]

$T_{1\rho}$ relaxation. The sensitivity of $T_{1\rho}$ relaxation to molecular motion is in a frequency range between T_1 and T_2; the slow (but not static) motional interactions between the confined water molecules and the macromolecules makes $T_{1\rho}$ less sensitive to the local fibril orientation. A unique feature (or complication) of $T_{1\rho}$ relaxation is its dependency on the strength of the spin-lock field (the radiofrequency field that locks the magnetisation in the transverse plane), a phenomenon termed as $T_{1\rho}$ dispersion (Figs 1e and 1f).[51] When the power of the spin-lock field is zero, $T_{1\rho}$ relaxation is identical to T_2 relaxation, which has all the features of T_2 anisotropy (note the similarity between $T_{1\rho}$ at 0 Hz in Fig. 1e and T_2 at 0° in Fig. 1c). With an increase of the spin-lock strength, $T_{1\rho}$ becomes less anisotropic, less depth-dependent, and has higher values. With a sufficiently high spin lock field (e.g., > 2000 Hz), the influence of the dipolar interaction to spin relaxation is sufficiently minimised to yield the measurement of a 'true' $T_{1\rho}$ (note the similarity of the $T_{1\rho}$ profiles at 2000 Hz in Figures 1e and 1f).

In most clinical MRI scanners, this 'sufficient spin-lock power' condition is never met, since most clinical MRI can only have the spin-lock field < 1000 Hz. The $T_{1\rho}$ value and profiles from the clinical MRI experiments are hence not 'pure' and still subject to the influence of the dipolar interaction (hence a small amount of the magic angle effect). Nevertheless, a reduced sensitivity to the dipolar interaction (and hence to the specimen orientation in the magnetic field) is a welcome feature in human imaging where the subject orientation in the magnet cannot be adjusted easily.

Diffusion. Self-diffusion quantifies random Brownian motion, which can be measured in μMRI by the incorporation of a pair of specific gradient pulses in the imaging sequence.[24] In early MRI literature, the value of self-diffusion was shown to be relatively uniform for most of the upper tissue and to decrease in the deep tissue. In addition, a small diffusion anisotropy (i.e., diffusion tensor[52,53]) was found in articular cartilage (Fig. 1g)[29,54] and found to occur at surface and deep portions of the tissue when the diffusion gradients were pointed to different directions (Fig. 1g). Several groups reported the increase of self-diffusion by about 20% to 30% upon trypsin-induced cartilage degradation.[55,56] A more comprehensive study of the role of the diffusion measurement in

cartilage degradation involved the use of several biochemical assays - each manipulated the GAG and collagen contents in cartilage distinctly differently.[57] The measurement suggested that the diffusion *was not* sensitive solely to the proteoglycan content of cartilage. Furthermore, analysis for collagen degradation established that diffusion does not depend solely on the collagen content of the tissue either. A likely mechanism to account for the increase in MRI diffusion values in both naturally occurring lesioned and biochemically-degraded cartilage is one in which microscopic holes are created that take the place of the macromolecules that have been degraded. Water fills these holes, and it is the enhanced freedom of water to diffuse within these holes that produces an increase in diffusion. This suggestion is supported by the observation that degenerated cartilage contains more water than normal tissue.[58] Compared with the widespread usage of relaxation measurement in MRI of cartilage, the potential for diffusion in MRI of cartilage may require further work.[59]

Multi-component relaxation. Since the dynamics of water molecules closely reflect the macromolecules they are associated (interacted) with, there must be more than one population of water in articular cartilage or any biological tissue. For example, one can speculate about the existence of the water associated with the collagen (the crystalline water), the water associated with the proteoglycan (the hydration water), and the relatively free water[60] (ignoring for the moment the exchanges among the different populations and the distribution of each population). Therefore, each relaxation time could have at least three components, each corresponding to one particular type of water population. In other words, the general practice in MRI that assigns only one value to T_1, T_2, or $T_{1\rho}$ at any pixel location is an approximation. While this is a correct statement in principle, whether one can measure all the components experimentally depends upon many practical factors. First, the individual components must be sufficiently different from each other for them to be resolved. Secondly, the exchange process among the spin populations must be sufficiently small to allow the differentiation of the individual components. Thirdly, the MRI instrument and experimental protocols must be capable of resolving the individual components. Finally, one must have an adequately small imaging voxel (i.e., high resolution) to avoid simple volume averaging of different morphological structures. What contributes to each of the four factors is beyond the scope of this brief review. Some succinct statements on multi-component relaxation can be made here.

1. Just as the fact that the notion of the *discrete* sub-tissue zones in articular cartilage is only a concept, the notion of three *discrete* water populations in cartilage is also only a concept. In reality, there are layers and layers of water molecules surrounding any macromolecule. Each outside layer would have weaker interactions with the macromolecule. In addition, the water molecules in each layer are also constantly moving to different layers. Hence, the distribution of any water population could never be a delta function, but would be a broad distribution peak. By the theory of relaxation physics, exchanges among these different populations do exist, which would further blur the distinction of the individual relaxation peaks.

2. Common protocols in clinical MRI and μMRI all have a minimum echo time of several milliseconds, during which the molecular information is not accessible. Most imaging experiments, hence, cannot resolve the shortest relaxation components (the water molecules that tightly interact or bind with the macromolecules). In addition, most relaxation protocols do not have sufficient resolutions to differentiate between different relaxation components. Consequently, almost all quantitative relaxation experiments by clinical MRI and μMRI in literature resolve only one relaxation component, which is influenced jointly by different amounts of all water populations. The only way to resolve multi-component relaxation in any imaging experiment is to reduce the min echo time[61,62] and to increase the relaxation resolution.[63-67]

3. The result of a multi-component relaxation experiment depends greatly upon the size and orientation of the imaging voxel. This is because any bulk (i.e., by spectroscopy) or low-resolution imaging must have its signal from a tissue volume that is large enough to contain many different structures, and hence, exhibiting several relaxation components. Only by μMRI can one measure multi-component relaxation coexisting intrinsically in the tissue. Recently, the role of dipolar interactions toward the measurements of multi-component relaxation in MRI of cartilage was noticed in several studies. Briefly, bovine nasal cartilage was found to have two T_2 components in some studies[67-69] and one T_2 component in some other studies.[63,65] Based on a 're-discovery' that nasal cartilage has a residual fibril anisotropy,[70] we recently provided the explanation that can unite the inconsistency in the literature[66]: there is a transition between multi-components and the mono-component in nasal cartilage, due to the influence of the residual collagen anisotropy and the strength of the spin-lock field.[66] These recent results demonstrate that the specimen orientation and experimental parameters must be considered for any multi-component analysis, even for nasal cartilage that is commonly considered homogenously structured.[71,72]

Factors that influence the cartilage appearance in MRI

In addition to the contrast factors that are important in MRI of cartilage, many experimental and tissue factors can also influence the appearance of articular cartilage in MRI and the detection of cartilage lesion by MRI. Detailed features of these experimental and tissue factors are beyond the scope of this review. Several factors are briefly discussed in this section.

The resolution scaling law in MRI of articular cartilage. The image resolution in MRI has non-trivial effects on the outcomes of the experiment. The dimension of an image voxel includes not only the common pixel resolution and slice thickness, but also the orientation of the universally pencil-shaped voxel in MRI.[10] The goal in any biomedical MRI is to tailor the dimensions and orientation of the image voxel to maximise the homogeneity of the molecular environment in each voxel, consequently reducing any artifacts due to partial volume averaging among different molecular populations (e.g., small lesion and large background tissue) within the same voxel. A resolution scaling law in MRI of cartilage[10] was formulated several years ago, which concluded that the transverse resolution in MRI for cartilage should ideally be 2% of the relative tissue depth per image pixel, which translates to about 40 μm for a 2 mm thick tissue (such as human knee or hip). This ideal resolution, at the present time, still poses challenges to whole-body MRI scanners. However, the societal importance of managing joint diseases, which is the number one cause of disabilities in the population,[3] is a sufficient motivation for all of us to work together to design higher-resolution MRI systems (e.g., extremity MRI) around this problem, and to develop novel MRI protocols (e.g., short echo-time protocols) that are exquisitely sensitive to the unique events in the early degradation of cartilage.

Strategies in image analysis for MRI of articular cartilage. Whether or not we have high resolution to resolve the details of articular cartilage, the layered-fan strategies in image analysis can improve the sensitivity and specificity of our MRI results. First, since T_2 anisotropy is always present in articular cartilage, we should always sub-divide the tissue in post-acquisition image analysis into several parallel layers, i.e., surface layer, middle layer, and deep layer. This layered analysis would always produce better results than obtaining a value that averages across the tissue depth. Secondly, instead of dividing the tissue into three equal-thickness layers, if the data allows, we should give the layers different thicknesses, with the first and second layers being the thinnest possible, and the last layer representing the thickest deep tissue. This way, one tries to separate and emphasise the differences among the three zones. Finally, instead of grouping all the values in each layer together, we should divide the tissue into several fan-segments (each at a different orientation with the magnetic field) and group all the values in any layer that have approximately the same orientation with respect to the magnetic field, in order to account for the consequences of the magic angle effect.

Imaging visualisation of the total tissues. Not all cartilage can be visualized in an MRI experiment. Since the echo time (TE) in common MRI pulse sequence is finite (typically 10 ms), it is difficult to image the portion of the tissue/water that has a T_2 relaxation time much shorter than the experimental TE. In cartilage MRI, the finite-width dark band between the soft tissue and bone might contain the invisible tissue. This is because the effects of TE and the relaxation time (e.g., T_2) are accounted for in MRI as a ratio: $\exp(-TE/T_2)$. For example, if the TE equals the T_2, the value of $\exp(-1)$ is 0.37, which means that this particular tissue/molecule component that has a T_2 relaxation time of 10 ms makes only a small contribution towards the total signal. If the ratio of TE over T_2 becomes -5, this portion of the tissue would contribute less than 1% towards the total signal, i.e., this portion of the tissue with a T_2 of 2 ms, when imaged under a TE of 10 ms, will be practically invisible on MRI. In order to image the total tissue, therefore, one needs to minimise the echo time of an MRI experiment.

Topographical variations of tissue properties. Cartilage is not a homogenous material.[73-82] This is certainly true for cartilage from different joints or from different species. Even for cartilage from different sampling sites of the same joint, a number of topographical variations in the chemical, physical, optical, and mechanical properties have been observed[83]; all of these topographical variations are also age-dependent,[84] which is probably a consequence of the load-bearing and motional patterns for particular joints and animals. Because of these topographical variations, one must keep in mind that a different sampling site within a relatively small area of the same joint surface may significantly alter the outcomes of the study, regardless of whether the study is morphological or mechanical, physical or chemical, *in vivo* or *in vitro*, clinical or in laboratory, or spectroscopic or imaging.

Surface fibril ambiguity. The orientational change of 90° for collagen fibrils between the SZ and the RZ is well accepted. This 90° orientational change, however, still leaves the freedom for the surface fibres to distribute themselves in any orientation in a 2D plane that is parallel with the articular surface: hence the observation of a "surface fibril ambiguity" in MRI literature.[38] Consequently, although the deep portion of the profiles of T_2 or $T_{1\rho}$ at small spin-lock powers is consistent among a group of cartilage specimens, the surface portion of the profiles of T_2 or $T_{1\rho}$ at small spin-lock frequencies can still fluctuate. Several years ago, a μMRI experiment was conducted purposefully to examine the surface fibril anisotropy.[85] A clear periodicity was found in the T_2 anisotropy at the superficial zone, which demonstrates that the distribution of the collagen fibrils in the superficial zone is not random. A collagen architecture model was formulated to interpret the experimental data, which suggests a potential mechanism that might be used to detect the fibrillation on the surface of articular cartilage *in vivo* and would provide an early indication of tissue degradation and joint disease.

Deformation of articular cartilage due to external loading. Since collagen orientation can significantly alter the intensity pattern of cartilage in MRI, a deformed collagen matrix in cartilage (which is natural to cartilage as a load-bearing tissue) must have some consequences in MRI of cartilage. Several μMRI studies during the last ten years

have documented the functional changes of the tissue due to the external loading. In essence, the value of the relaxation will decrease in loaded cartilage. In addition, contrary to what has been observed in normal (unloaded) cartilage at the magic angle (Fig. 1c), the loaded tissue at the magic angle no longer appears homogenous. Instead, there is a distinctly laminar appearance at the magic angle, which contains a strain-dependent dark band.[86,87] This work implies that compression can become a controllable mechanism in MRI to induce new image contrast and can be, in every sense, a functional study of the tissue's structures and properties – compression may be used to study the damage to the fine structure of the collagen matrix, and the reduction of the proteoglycan contents in cartilage. This topic is being studied actively in our lab in recent years.[88-90] MRI of loaded cartilage has also been realised in recent years in clinical MRI.[91,92]

Cartilage lesions. The theory of MRI physics implies that the values of the relaxation and diffusion would increase if the water molecules were in a less viscous and freer environment. The mechanisms of cartilage degradation leads to the knowledge that cartilage would have less proteoglycan, more water, and bigger spaces between the fibrils during the early stages of tissue degradation. Consequently, one can conclude that the values of the relaxations and diffusion would increase when the tissue is degraded (provided that the fibril matrix is still intact), which has indeed been observed in T_2 relaxation,[63,93] $T_{1\rho}$ relaxation[44-48,51] and self-diffusion.[55-62]

The accuracy and sensitivity of these molecular-level imaging biomarkers, however, are less than ideal at the present time[4] due to some of the factors discussed previously in this review. By reducing the size of the imaging voxel, one can improve the homogeneity of the molecular environment, consequently reducing any artifacts due to partial volume averaging, competing mechanisms, and topographical variations. By reducing the echo time and improving the MRI system, one can reduce the dipolar interaction, consequently reducing orientational influences to T_2 and $T_{1\rho}$. Finally, by using multidisciplinary techniques, one can discriminate among the various factors and changes and their influence on the functional integrity of cartilage as a load-bearing biological tissue. This would provide critical information towards the development of novel methods for early detection and effective monitoring of the aetiology of cartilage diseases at both clinical and molecular levels.

Conclusions

In contrast to most clinical MRI studies of cartilage for which the imaging resolution is about several hundreds of microns or poorer, μMRI can have a transverse resolution as fine as tens of microns across the depth of the cartilage tissue. At the present time, this high resolution is not possible in clinical MRI. Hence, μMRI at the present stage is a basic research tool for the benches in the labs. Given the fact that μMRI shares the same physics and engineering principles with clinical MRI, however, μMRI study of animal models of human diseases presents itself as a logical and ideal combination. μMRI has direct and immediate clinical relevance in that one can identify the parameter or procedure that might be useful clinically. In addition, since μMRI resolutions sit between those of ultrastructural optical/electronic imaging and clinical MRI, the μMRI projects provide an ideal intermediate-resolution platform to coarse-grain the ultrastructural results for an eventual clinical application.

We have been studying articular cartilage for nearly 20 years in our lab, initially using μMRI because it can map the physical properties of viable cartilage in its near-native environment. In the later 1990s, we started to incorporate PLM (polarised light microscopy) in our work, because PLM (the gold standard in histology) can image the collagen organisation,[39,90,93] which modulates the μMRI signal. As our projects progressed, we needed to image the molecular concentrations in the early lesion cartilage as directly as possible, at high resolutions. For this reason, since 2005, we started to use FTIRI (Fourier-transform infrared imaging) in our work. FTIRI is sensitive to the vibration of dipole moments of chemical bonds in tissue.[94-97] In addition to these high-resolution imaging tools, we also employ several biomechanical and biochemical methods – each measures a unique aspect of the tissue's bulk properties and can be correlated with the spatially resolved changes in imaging. This multidisciplinary research approach is a recognition that many of today's biomedical problems are best addressed using multi-disciplinary techniques; each method has its own scientific merit.[19] In view of the molecular and ultrastructural changes due to early diseases and the interdependent structure-function-property relationships in tissue, applying multi-disciplinary techniques can discriminate among the various factors and changes and their influence on the functional integrity of cartilage as a load-bearing material. Even though neither μMRI nor PLM nor FTIRI has the resolution to identify individual collagen fibrils or other molecules, a multidisciplinary micro-imaging approach can identify subtle changes in the morphological structure and molecular concentration in cartilage due to natural lesions and mechanical loading, enabling the monitoring and prediction of early changes in tissue that lead to cartilage degradation as a clinical disease.

The author is grateful to the R01 grant from the National Institutes of Health (NIH AR 052353), to the students and staff in the laboratory who undertook the original cartilage imaging work, to Dr C. Les (Henry Ford Hospital, Detroit) for stimulating discussions, to Miss A. Xia (College of Engineering, University of Michigan) and Ms C. Searight (Department of Physics, Oakland University) for editorial comments on the manuscript.

References

1. **Helmick CG, Felson DT, Lawrence RC, et al.** Estimates of the prevalence of arthritis and other rheumatic conditions in the United States: Part I. *Arthritis Rheum* 2008;58:15–25.
2. **Lawrence RC, Felson DT, Helmick CG, et al.** Estimates of the prevalence of arthritis and other rheumatic conditions in the United States: Part II. *Arthritis Rheum* 2008;58:26–35.

3. **Centers for Disease Control and Prevention.** Prevalence and most common causes of disability among adults (United States, 2005). *Morbidity and Mortality Weekly Report* May 1, 2009;58:421–426. http://www.cdc.gov/mmwr/preview/mmwrhtml/mm5816a2.htm (date last accessed 26 September 2012).
4. **Burstein D, Gray ML.** Is MRI fulfilling its promise for molecular imaging of cartilage in arthritis? *Osteoarthritis Cartilage* 2006;14:1087–1090.
5. **Schaible HG.** Mechanisms of chronic pain in osteoarthritis. *Curr Rheumatol Rep* 2012;14:549–556.
6. **Parks EL, Geha PY, Baliki MN, et al.** Brain activity for chronic knee osteoarthritis: dissociating evoked pain from spontaneous pain. *Eur J Pain* 2011;15:843–841.
7. **Sofat N, Ejindu V, Kiely P.** What makes osteoarthritis painful?: the evidence for local and central pain processing. *Rheumatology (Oxford)* 2011;50:2157–2165.
8. **Inoue R, Ishibashi Y, Tsuda E, et al.** Knee osteoarthritis, knee joint pain and aging in relation to increasing serum hyaluronan level in the Japanese population. *Osteoarthritis Cartilage* 2011;19:51–57.
9. **Goddard NJ, Gosling PT.** Intra-articular fluid pressure and pain in osteoarthritis of the hip. *J Bone Joint Surg [Br]* 1988;70-B:52–55.
10. **Xia Y.** Resolution 'scaling law' in MRI of articular cartilage. *Osteoarthritis Cartilage* 2007;15:363–365.
11. **Xia Y.** Contrast in NMR imaging and microscopy. *Concepts Magn Reson* 1996;8:205–225.
12. **Hunziker EB, Quinn TM, Häuselmann HJ.** Quantitative structural organization of normal adult human articular cartilage. *Osteoarthritis Cartilage* 2002;10:564–572.
13. **Venn M, Maroudas A.** Chemical composition and swelling of normal and osteoarthritic femoral head cartilage: I: Chemical composition. *Ann Rheum Dis* 1977;36:121–129.
14. **Maroudas A, Bayliss MT, Venn M.** Further studies on the composition of human femoral head cartilage. *Ann Rheum Dis* 1980;39:514–534.
15. **Clarke IC.** Articular cartilage: a review and scanning electron microscope study: 1: The interterritorial fibrillar architecture. *J Bone Joint Surg [Br]* 1971;53-B:732–750.
16. **Bayliss MT, Venn M, Maroudas A, Ali SY.** Structure of proteoglycans from different layers of human articular cartilage. *Biochem J* 1983;209:387–400.
17. **Maroudas A, Wachtel EJ, Grushko G, Katz EP, Weinberg P.** The effect of osmotic and mechanical pressures on water partitioning in articular cartialge. *Biochim Biophys Acta* 1991;1073:285–294.
18. **Mow VC, Guo XE.** Mechano-electrochemical properties of articular cartilage: their inhomogeneities and anisotropies. *Ann Rev Biomed Eng* 2002;4:175–209.
19. **Xia Y.** Averaged and depth-dependent anisotropy of articular cartilage by microscopic imaging. *Semin Arthritis Rheum* 2008;37:317–327.
20. **Callaghan PT.** *Principles of nuclear magnetic resonance microscopy.* Oxford: Oxford University Press, 1991.
21. **Blümich B, Kuhn W.** *Magnetic resonance microscopy: methods and application in materials science, agriculture and biomedicine.* Weinheim: VCH, 1992.
22. **Blümler P, Blümich B, Botto R, Fukushima E, eds.** *Spatially resolved magnetic resonance: methods, materials, medicine, biology, rheology, geology, ecology, hardware.* Weinheim: Wiley-VCH, 1998.
23. **Jenner CF, Xia Y, Eccles CD, Callaghan PT.** Circulation of water within wheat grain revealed by nuclear magnetic resonance micro-imaging. *Nature* 1988;336:399–402.
24. **Callaghan PT, Xia Y.** Velocity and diffusion imaging in dynamic NMR microscopy. *J Magn Reson* 1991;91:326–352.
25. **Xia Y, Farquhar T, Burton-Wurster N, Lust G.** Origin of cartilage laminae in MRI . *J Magn Reson Imaging* 1997;7:887–894.
26. **Slichter CP.** *Principles of magnetic resonance.* Berlin: Springer-Verlag, 1992.
27. **Xia Y.** Relaxation anisotropy in cartilage by NMR microscopy (muMRI) at 14-micron resolution. *Magn Reson Med* 1998;39:941–949.
28. **Muir H.** Proteoglycans as organizers of the intercellular matrix. *Biochem Soc Trans* 1983;11:613–622.
29. **Xia Y, Farquhar T, Burton-Wurster N, Jelinski LW.** Microscopic MRI studies of cartilage. *Orthop Trans* 1994;18:403–404.
30. **Tyrrell RL, Gluckert K, Pathria M, Modic MT.** Fast three-dimensional MR imaging of the knee: comparison with arthroscopy. *Radiology* 1988;166:865–872.
31. **Lehner KB, Rechl HP, Gmeinwieser JK, et al.** Structure, function, and degeneration of bovine hyaline cartilage: assessment with MR imaging in vitro. *Radiology* 1989;170:495–499.
32. **Hayes CW, Sawyer RW, Conway WF.** Patellar cartilage lesions: in vitro detection and staging with MR imaging and pathologic correlation. *Radiology* 1990;176:479–483.
33. **Modl JM, Sether LA, Haughton VM, Kneeland JB.** Articular cartilage correlation of histologic zones with signal intensity at MR Imaging. *Radiology* 1991;181:853–855.
34. **Hayes CW, Parellada JA.** The magic angle effect in musculoskeletal MR imaging. *Top Magn Reson Imaging* 1996;8:51–56.
35. **Rubenstein JD, Kim JK, Morava-Protzner I, Stanchev PL, Henkelman RM.** Effects of collagen orientation on MR imaging characteristics of bovine articular cartilage. *Radiology* 1993;188:219–226.
36. **Xia Y.** Magic angle effect in MRI of articular cartilage: a review. *Invest Radiol* 2000;35:602–621.
37. **Bydder M, Rahal A, Fullerton GD, Bydder GM.** The magic angle effect: a source of artifact, determinant of image contrast, and technique for imaging. *J Magn Reson Imaging* 2007;25:290–300.
38. **Xia Y, Moody J, Alhadlaq H.** Orientational dependence of T2 relaxation in articular cartilage: a microscopic MRI (microMRI) study. *Magn Reson Med* 2002;48:460–469.
39. **Xia Y, Moody J, Burton-Wurster N, Lust G.** Quantitative in situ correlation between microscopic MRI and polarized light microscopy studies of articular cartilage. *Osteoarthritis Cartilage* 2001;9:393–406.
40. **Zheng S, Xia Y, Bidthanapally A, et al.** Damages to the extracellular matrix in articular cartilage due to cryopreservation by microscopic magnetic resonance imaging and biochemistry. *Magn Reson Imaging* 2009;27:648–655.
41. **Xia Y, Zheng S.** Reversed laminar appearance of articular cartilage by T1-weighting in 3D fat-suppressed spoiled gradient recalled echo (SPGR) imaging. *J Magn Reson Imaging* 2010;32:733–737.
42. **McCauley TR, Disler DG.** MR imaging of articular cartilage. *Radiology* 1998;209:629–640.
43. **Bashir A, Gray ML, Burstein D.** Gd-DTPA2- as a measure of cartilage degradation. *Magn Reson* Med 1996;36:665–673.
44. **Trattnig S, Mlynárik V, Breitenseher M, et al.** MRI visualization of proteoglycan depletion in articular cartilage via intravenous administration of Gd-DTPA. *Magn Reson Imaging* 1999;17:577–583.
45. **Nieminen MT, Rieppo J, Silvennoinen J, et al.** Spatial assessment of articular cartilage proteoglycans with Gd-DTPA-enhanced T1 imaging. *Magn Reson Med* 2002;48:640–648.
46. **Nieminen MT, Töyräs J, Laasanen MS, et al.** Prediction of biomechanical properties of articular cartilage with quantitative magnetic resonance imaging. *J Biomech* 2004;37:321–328.
47. **Samosky JT, Burstein D, Eric Grimson W, et al.** Spatially-localized correlation of dGEMRIC-measured GAG distribution and mechanical stiffness in the human tibial plateau. *J Orthop Res* 2005;23:93–101.
48. **Wedig M, Bae W, Temple M, Sah R, Gray M.** [GAG] profiles in "normal" human articular cartilage. Procs Orthopedic Research Society Meeting, Washington DC, 2005.
49. **Xia Y, Zheng S, Bidthanapally A.** Depth-dependent profiles of glycosaminoglycans in articular cartilage by microMRI and histochemistry. *J Magn Reson Imaging* 2008;28:151–157.
50. **Zheng S, Xia Y.** The impact of the relaxivity definition on the quantitative measurement of glycosaminoglycans in cartilage by the MRI dGEMRIC method. *Magn Reson Med* 2010;63:25–32.
51. **Wang N, Xia Y.** Depth and orientational dependencies of MRI T(2) and T(1rho) sensitivities towards trypsin degradation and Gd-DTPA(2-) presence in articular cartilage at microscopic resolution. *Magn Reson Imaging* 2012;30:361–370.
52. **Basser PJ, Jones DK.** Diffusion-tensor MRI: theory, experimental design and data analysis: a technical review. *NMR Biomed* 2002;15:456–467.
53. **Momot KI.** Diffusion tensor of water in model articular cartilage. *Eur Biophys J* 2011;40:81–91.
54. **Xia Y, Farquhar T, Burton-Wurster N, Ray E, Jelinski LW.** Diffusion and relaxation mapping of cartilage-bone plugs and excised disks using microscopic magnetic resonance imaging. *Magn Reson Med* 1994;31:273–282.
55. **Burstein D, Gray ML, Hartman AL, Gipe R, Foy BD.** Diffusion of small solutes in cartilage as measured by nuclear magnetic resonance (NMR) spectroscopy and imaging. *J Orthop Res* 1993;11:465–478.
56. **Xia Y, Tso D, Farquhar T, Burton-Wurster N, Jelinski LW.** Microscopic MRI studies of cartilage. Procs Orthopedic Research Society Meeting, New Orleans, 1994.
57. **Xia Y, Farquhar T, Burton-Wurster N, et al.** Self-diffusion monitors degraded cartilage. *Arch Biochem Biophys* 1995;323:323–328.
58. **Burton-Wurster N, Hui-Chou CS, Greisen HA, Lust G.** Reduced deposition of collagen in the degenerated articular cartilage of dogs with degenerative joint disease. *Biochem Biophys Acta* 1982;718:74–84.
59. **Deng X, Farley M, Nieminen MT, Gray M, Burstein D.** Diffusion tensor imaging of native and degenerated human articular cartilage. *Magn Reson Imaging* 2007;25:168–171.
60. **Fullerton GD, Potter JL, Dornbluth NC.** NMR relaxation of protons in tissues and other macromolecular water solutions. *Magn Reson Imaging* 1982;1:209–226.
61. **Du J, Diaz E, Carl M, et al.** Ultrashort echo time imaging with bicomponent analysis. *Magn Reson Med* 2012;67:645–649.
62. **Qian Y, Williams AA, Chu CR, Boada FE.** Multicomponent T2* mapping of knee cartilage: technical feasibility ex vivo. *Magn Reson Med* 2010;64:1426–1431.
63. **Zheng S, Xia Y.** Multi-components of T2 relaxation in ex vivo cartilage and tendon. *J Magn* Reson 2009;198:188–196.

64. **Reiter DA, Lin PC, Fishbein KW, Spencer RG.** Multicomponent T2 relaxation analysis in cartilage. *Magn Reson Med* 2009;61:803–809.
65. **Zheng S, Xia Y.** On the measurement of multi-component T2 relaxation in cartilage by MR spectroscopy and imaging. *Magn Reson Imaging* 2010;28:537–555.
66. **Wang N, Xia Y.** Dependencies of multi-component T2 and T1rho relaxation on the anisotropy of collagen fibrils in bovine nasal cartilage. *J Magn Reson* 2011;212:124–132.
67. **Reiter DA, Roque RA, Lin PC, et al.** Mapping proteoglycan-bound water in cartilage: Improved specificity of matrix assessment using multiexponential transverse relaxation analysis. *Magn Reson Med* 2011;65:377–384.
68. **Keinan-Adamsky K, Shinar H, Navon G.** The effect of detachment of the articular cartilage from its calcified zone on the cartilage microstructure, assessed by 2H-spectroscopic double quantum filtered MRI. *J Orthop Res* 2005;23:109–117.
69. **Reiter DA, Peacock A, Spencer RG.** Effects of frozen storage and sample temperature on water compartmentation and multiexponential transverse relaxation in cartilage. *Magn Reson Imaging* 2011;29:561–567.
70. **Xia Y, Zheng S, Szarko M, Lee J.** Anisotropic properties of bovine nasal cartilage. *Microsc Res Tech* 2012;75:300–306.
71. **Glasgold MJ, Kato YP, Christiansen D, et al.** Mechanical properties of septal cartilage homografts. *Otolaryngol Head Neck Surg* 1988;99:374–379.
72. **Grellmann W, Berghaus A, Haberland EJ, et al.** Determination of strength and deformation behavior of human cartilage for the definition of significant parameters. *J Biomed Mater Res A* 2006;78:168–174.
73. **Weiss C, Rosenberg L, Helfet AJ.** An ultrastructural study of normal young adult human articular cartilage. *J Bone Joint Surg [Am]* 1968;50-A:663–674.
74. **Meachim G.** Effect of age on the thickness of adult articular cartilage at the shoulder joint. *Ann Rheum Dis* 1971;30:43–46.
75. **Zimny ML, Redler I.** Morphological variations within a given area of articular surface of cartilage. *Z Zellforsch Mikrosk Anat* 1974;147:163–167.
76. **Kincaid SA, Van Sickle DC.** Regional histochemical and thickness variations of adult canine articular cartilage. *Am J Vet Res* 1981;42:428–432.
77. **Slowman SD, Brandt KD.** Composition and glycosaminoglycan metabolism of articular cartilage from habitually loaded and habitually unloaded sites. *Arthritis Rheum* 1986;29:88–94.
78. **Kiviranta I, Tammi M, Jurvelin J, Helminen HJ.** Topographical variation of glycosaminoglycan content and cartilage thickness in canine knee (stifle) joint cartilage: application of the microspectrophotometric method. *J Anat* 1987;150:265–276.
79. **Korvick D, Athanasiou K.** Variations in the mechanical properties of cartilage from the canine scapulohumeral joint. *Am J Vet Res* 1997;58:949–953.
80. **Farquhar T, Bertram J, Todhunter RJ, Burton-Wurster N, Lust G.** Variations in composition of cartilage from the shoulder joints of young adult dogs at risk for developing canine hip dysplasia. *J Am Vet Med Assoc* 1997;210:1483–1485.
81. **Fragonas E, Mlynárik V, Jellús V, et al.** Correlation between biochemical composition and magnetic resonance appearance of articular cartilage. *Osteoarthritis Cartilage* 1998;6:24–32.
82. **Brama PA, TeKoppele JM, Bank RA, van Weeren PR, Barneveld A.** Influence of site and age on biochemical characteristics of the collagen network of equine articular cartilage. *Am J Vet Res* 1999;60:341–345.
83. **Xia Y, Moody J, Alhadlaq H, Burton-Wurster N, Lust G.** Characteristics of topographical heterogeneity of articular cartilage over the joint surface of a humeral head. *Osteoarthritis Cartilage* 2002;10:370–380.
84. **Xia Y, Moody J, Alhadlaq H, Hu JN.** Imaging the physical and morphological properties of a multi-zone young articular cartilage at microscopic resolution. *J Magn Reson Imaging* 2003;17:365–374.
85. **Zheng S, Xia Y.** The collagen fibril structure in the superficial zone of articular cartilage by μMRI. *Osteoarthritis Cartilage* 2009;17:1519–1528.
86. **Alhadlaq H, Xia Y.** The structural adaptations in compressed articular cartilage by microscopic MRI (microMRI) T(2) anisotropy. *Osteoarthritis Cartilage* 2004;12:887–894.
87. **Alhadlaq HA, Xia Y.** Modifications of orientational dependence of microscopic magnetic resonance imaging T(2) anisotropy in compressed articular cartilage. *J Magn Reson Imaging* 2005;22:665–673.
88. **Alhadlaq HA, Xia Y, Hansen FM, Les CM, Lust G.** Morphological changes in articular cartilage due to static compression: polarized light microscopy study. *Connect Tissue Res* 2007;48:76–84.
89. **Xia Y, Alhadlaq H, Ramakrishnan N, et al.** Molecular and morphological adaptations in compressed articular cartilage by polarized light microscopy and Fourier-transform infrared imaging. *J Struct Biol* 2008;164:88–95.
90. **Xia Y, Wang N, Lee J, Badar F.** Strain-dependent T1 relaxation profiles in articular cartilage by MRI at microscopic resolutions. *Magn Reson Med* 2011;65:1733–1737.
91. **Gold GE, Besier TF, Draper CE, et al.** Weight-bearing MRI of patellofemoral joint cartilage contact area. *J Magn Reson Imaging* 2004;20:526–530.
92. **Stehling C, Souza RB, Graverand MP, et al.** Loading of the knee during 3.0 T MRI is associated with significantly increased medial meniscus extrusion in mild and moderate osteoarthritis. *Eur J Radiol* 2012;81:1839–1845.
93. **Alhadlaq H, Xia Y, Moody JB, Matyas J.** Detecting structural changes in early experimental osteoarthritis of tibial cartilage by microscopic magnetic resonance imaging and polarized light microscopy. *Ann Rheum Dis* 2004;63:709–717.
94. **Xia Y, Ramakrishnan N, Bidthanapally A.** The depth-dependent anisotropy of articular cartilage by Fourier-transform infrared imaging (FTIRI). *Osteoarthritis Cartilage* 2007;15:780–788.
95. **Ramakrishnan N, Xia Y, Bidthanapally A.** Polarized IR microscopic imaging of articular cartilage. *Phys Med Biol* 2007;52:4601–4614.
96. **Yin JH, Xia Y.** Macromolecular concentrations in bovine nasal cartilage by fourier transform infrared imaging and principal component regression. *Appl Spectrosc* 2010;64:1199–1208.
97. **Yin JH, Xia Y, Ramakrishnan N.** Depth-dependent anisotropy of proteoglycan in articular cartilage by Fourier transform infrared imaging. *Vib Spectrosc* 2011;57:338–341.

Funding statement:

- This work was supported by a NIH R01 Grant (AR052353).

Author contributions:

- Y. Xia: Researched and wrote the paper

ICMJE Conflict of Interest:

- None declared